https://doi.org/10.15407/ujpe68.6.383

I.V. PYLYUK, M.P. KOZLOVSKII, O.A. DOBUSH

Institute for Condensed Matter Physics, Nat. Acad. of Sci. of Ukraine
(1, Svientsitskii Str., Lviv 79011, Ukraine; e-mail: piv@icmp.lviv.ua)

THERMODYNAMIC QUANTITIES OF MORSE FLUIDS IN THE SUPERCRITICAL REGION

The critical point parameters for liquid alkali metals (sodium and potassium) are calculated accounting for the non-Gaussian order parameter fluctuations and the Morse interaction potential. The behavior of the isothermal compressibility, density fluctuations, and thermal expansion for sodium is studied in the supercritical temperature region. A significant increase in the isothermal compressibility and the density fluctuations near the critical point indicates a substantial density sensitivity to tiny pressure fluctuations. The thermal expansion coefficient for various fixed pressure values shows a typical gas decrease with increasing supercritical temperature. The Widom line separating the gaseous and liquid structures of the fluid at temperatures above the critical one is represented. Note that our calculations are valid in a small neighborhood of the critical point, which is problematic for theoretical and experimental studies.

K e y w o r d s: Morse interaction potential, critical point, thermodynamic potential, isothermal compressibility, density fluctuations, thermal expansion.

1. Introduction

The theoretical and experimental study of the behavior of simple and multicomponent liquid systems in vicinities of their critical points (see, for example, works [1–9]) remains an actual task.

In the last decades, the interest in supercritical fluids, the study of their unique properties, and their application in different fields of science and technology has been growing steadily [6, 7, 10–12]. The reason for the persistent interest in describing the nature of phase transitions and critical phenomena in liquid systems is that near-critical fluids are the most suitable objects for modeling a class of systems with many strongly interacting degrees of freedom [13, 14]. On the other hand, the supercritical fluids are increasingly widely used in various technological processes due to their specific properties [15]. In this regard, constructing the equation of state of supercritical fluids becomes a crucial applied problem.

C i t a t i o n: Pylyuk I.V., Kozlovskii M.P., Dobush O.A. Thermodynamic quantities of Morse fluids in the supercritical region. *Ukr. J. Phys.* **68**, No. 6, 383 (2023). https://doi.org/10.15407/ujpe68.6.383.

Ц и т у в а н н я: Пилюк І.В., Козловський М.П., Добуш О.А. Термодинамічні величини плинів Морзе в надкритичній області. *Укр. фіз. журн.* **68**, №6, 383 (2023).

The theoretical calculation of the equation of state by the methods of statistical physics is complicated by the correct consideration of the interparticle interaction, which is complex in structure. In calculations, we use simplified models. The scope of these models is limited and established in each specific case. For this purpose, the internal characteristics of the model are taken into account, or the model solutions are compared with more accurate solutions or experimental results.

In this paper, we will perform the microscopic description and investigation of the fluid critical behavior within the framework of the grand canonical ensemble. This task is essential, since the presence of a chemical potential in the grand canonical ensemble leads to an adequate representation of existing atomic and molecular systems. Only this thermodynamic parameter is responsible for the exchange of constituents between different parts of the system and with the environment. Moreover, it quantitatively describes the tendency of a thermodynamic system to establish compositional equilibrium.

The object of the present study is the Morse fluid in the supercritical region. The previously proposed approach for the microscopic description of the critical behavior of Morse liquids based on the cell fluid model is applied to alkali metals (sodium and potassium).

2. Cell Fluid Model and the Interaction Potential

In this paper, a cell fluid model is used for studying the behavior of a simple fluid in a vicinity of the liquid–gas critical point. We consider a system of N interacting particles in the volume V conditionally divided into N_v cells ($V = vN_v$, $v = c^3$ is the cell volume, and c is the linear size of a cell) [16–18]. In contrast to a cell gas model (where a cell is assumed to contain only one particle or be empty) [19, 20], in our approach, a cell may contain more than one particle [21, 22]. Besides, the distance between the cells is introduced instead of the distance between the particles.

The grand partition function of the cell fluid model within the framework of the grand canonical ensemble is as follows [17, 18]:

$$\Xi = \sum_{N=0}^{\infty} \frac{(z)^N}{N!} \int\limits_V (dx)^N \exp\left[-\frac{\beta}{2} \sum_{\mathbf{l}_1,\mathbf{l}_2 \in \Lambda} \tilde{U}_{l_{12}} \rho_{\mathbf{l}_1}(\eta) \rho_{\mathbf{l}_2}(\eta) \right]. \tag{1}$$

Here, $z = e^{\beta\mu}$ is the activity, $\beta = 1/(kT)$ is the inverse temperature, and μ is the chemical potential. The integration with respect to coordinates of all the particles $x_i = (x_i^{(1)}, x_i^{(2)}, x_i^{(3)})$ is noted as $\int_V (dx)^N = \int_V dx_1 \cdots \int_V dx_N$, and $\eta = \{x_1, ..., x_N\}$ is the set of coordinates. The interaction potential $\tilde{U}_{l_{12}}$ is a function of the distance $l_{12} = |\mathbf{l}_1 - \mathbf{l}_2|$ between cells. Each vector $\mathbf{l}_i$ belongs to the set

$$\Lambda = \Big\{ \mathbf{l} = (l_1, l_2, l_3) | l_i = c m_i; \quad m_i = 1, 2, ..., N_a; \\ i = 1, 2, 3; \quad N_v = N_a^3 \Big\}, \tag{2}$$

where N_a is the number of cells along each axis. The occupation numbers of cells

$$\rho_{\mathbf{l}}(\eta) = \sum_{x \in \eta} I_{\Delta_{\mathbf{l}}(x)} \tag{3}$$

appearing in Eq. (1) are defined by the characteristic functions (indicators)

$$I_{\Delta_{\mathbf{l}}(x)} = \begin{cases} 1, & \text{if } x \in \Delta_{\mathbf{l}} \\ 0, & \text{if } x \notin \Delta_{\mathbf{l}}, \end{cases} \tag{4}$$

which identify the particles in each cubic cell $\Delta_{\mathbf{l}} = (-c/2, c/2]^3 \subset \mathbb{R}^3$ and their contribution to the interaction of the model. Henceforth, we choose the Morse potential as the interaction potential $\tilde{U}_{l_{12}}$:

$$\begin{aligned} &\tilde{U}_{l_{12}} = \Psi_{l_{12}} - U_{l_{12}}; \\ &\Psi_{l_{12}} = D e^{-2(l_{12}-1)/\alpha_R}, \\ &U_{l_{12}} = 2D e^{-(l_{12}-1)/\alpha_R}. \end{aligned} \tag{5}$$

Here, $\Psi_{l_{12}}$ and $U_{l_{12}}$ are the repulsive and attractive parts of the potential, respectively, and $\alpha_R = \alpha/R_0$ (α is the effective interaction radius). The parameter R_0 corresponds to the minimum of the function $\tilde{U}_{l_{12}}$, and D determines the depth of a potential well. Note that the R_0-units are used for the length measuring for convenience. As a result, R_0- and R_0^3-units are used for the linear size of each cell c and volume v, respectively.

3. Thermodynamic Potential of the Model and the Equation of State

The basic idea of the thermodynamic potential calculation near the critical point within the approach of collective variables (CV) [23, 24] lies in the separate inclusion of contributions from short-wave and long-wave modes of order parameter oscillations. The short-wave modes are characterized by a renormalization group (RG) symmetry and described by a non-Gaussian measure density. They correspond to the critical regime region observed above and below the critical temperature T_c. In this case, the RG method is used. We integrate the grand partition function of the cell fluid model over the layers of the CV phase space (see [17]). The corresponding RG transformation can be related to the Wilson type. Although, like the Wilson approach, the CV method exploits the RG ideas, it is based on the use of a non-Gaussian density of measure. The main feature is the integration of short-wave oscillation modes, which is generally done without using perturbation theory. As a result, we obtained the recurrence relations between the coefficients of the effective quartic measure densities, their solutions, and the equation for the critical temperature [17]. Including the short-wave oscillation modes leads to a renormalization of the dispersion of the distribution describing long-wave modes. In the case of $T > T_c$, these long-wave modes correspond to the region of the limiting Gaussian regime. We consider the contribution from the long-wave modes of oscillations to the thermodynamic potential of the cell fluid model in the way, which is qualitatively different from the

method of calculating the short-wave part of the thermodynamic potential. The calculation of this contribution is based on the use of the Gaussian measure density as the basis one. Here, we have developed a direct method of calculation with the results obtained by accounting for the short-wave modes as initial parameters.

The complete expression for the thermodynamic potential

$$\Omega = \Omega_a + \Omega_s^{(+)} + \Omega_0^{(+)} \tag{6}$$

is obtained by summing up the contributions from short-wave and long-wave modes of order parameter oscillations. The terms

$$\Omega_a = -kTN_v\left(\gamma_{01} + \gamma_{02}\tau + \gamma_{03}\tau^2\right) + \Omega_{01} \tag{7}$$

and

$$\Omega_s^{(+)} = -kTN_v\gamma_s^{(+)}(\tilde{h}^2 + h_c^2)^{\frac{d}{d+2}} \tag{8}$$

correspond to the analytic and nonanalytic parts of the thermodynamic potential, respectively. The third term in Eq. (6), associated with the CV ρ_0, is defined as

$$\Omega_0^{(+)} = -kTN_v\Big[e_0^{(+)}\tilde{h}(\tilde{h}^2 + h_c^2)^{\frac{d-2}{2(d+2)}} - e_2^{(+)}(\tilde{h}^2 + h_c^2)^{\frac{d}{d+2}}\Big]. \tag{9}$$

The quantity Ω_{01} and the coefficients appearing in Eqs. (7)–(9) can be found in work [17]. The quantity $\tilde{h}$ is proportional to the renormalized chemical potential, and the quantity h_c is characterized by the renormalized relative temperature, $\tau = (T - T_c)/T_c$ is the relative temperature, $d = 3$ is the space dimension.

In the course of describing the behavior of the supercritical fluid, we obtained and investigated a nonlinear equation connecting the average density $\bar{n}$ and the renormalized chemical potential M. The quantity M is expressed by the initial chemical potential μ (hereafter, consider M the chemical potential). This equation can be represented as [17]

$$b_3^{(+)}M^{1/5} = \bar{n} - n_g + M, \tag{10}$$

where

$$b_3^{(+)} = \left(\frac{b_1^{(+)}}{b_2^{(+)}}\right)^{1/5}\sigma_{00}^{(+)},$$

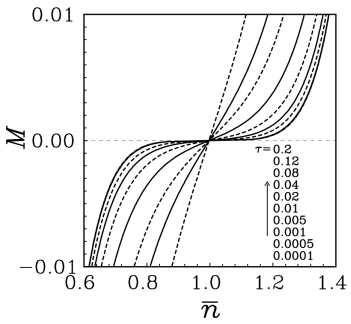

Fig. 1. Dependence of the chemical potential M on the average density $\bar{n}$ for various values of the relative temperature τ. The arrow points on the correspondence between τ and curves of M at the transition from down to up in the first quadrant of the coordinate plane

$$b_1^{(+)} = (\beta W(0))^{1/2}, \qquad b_2^{(+)} = \frac{\alpha}{(1+\alpha^2)^{1/2}}. \tag{11}$$

Here, $W(0)$ is the Fourier transform of the effective interaction potential at the zero value of the wave vector, and n_g is determined by the coefficients of the initial expression for the grand partition function. The coefficient $\sigma_{00}^{(+)}$ is a function of the quantity α, which is defined as the ratio of the renormalized chemical potential to the renormalized relative temperature. Equation (10) allows for tracing the chemical potential M ($M \ll 1$) as a function of $\bar{n}$ at different fixed values of the relative temperature τ (see Fig. 1). Note that all the graphic material represented in this paper is for the parameters of the Morse interaction potential taken from [18], which correspond to the data for sodium [25]. Work [18] also contains a set of parameters for potassium. In particular, we have $R_0/\alpha = 2.9544$ for sodium and $R_0/\alpha = 3.0564$ for potassium.

The expression for the logarithm of the grand partition function (or the thermodynamic potential $\Omega = -kT\ln\Xi$) derived in [17] for the cell fluid model at $T > T_c$ makes it possible to obtain the pressure P as a function of the temperature T and the chemical potential μ using the well-known equation

$$PV = kT\ln\Xi. \tag{12}$$

Having the grand partition function, we can also find the average number of particles

$$\bar{N} = \frac{\partial\ln\Xi}{\partial\beta\mu}. \tag{13}$$

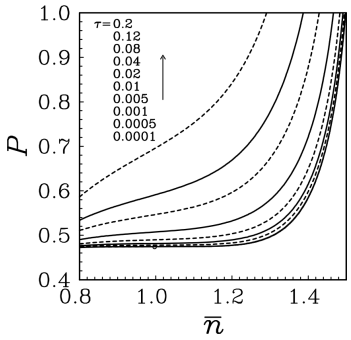

Fig. 2. Dependence of the pressure P on the average density $\bar{n}$ at different fixed temperatures τ. The critical point ($\bar{n}_c = 0.997$, $P_c = 0.474$) is marked by the symbol ∘

Dimensionless critical temperature kT_c, average density $\bar{n}_c$, and pressure P_c, obtained for sodium (Na) and potassium (K) on the basis of the cell fluid model (CFM) in the zero mode approximation (ZMA) [26] (see the first row) and in the ρ^4 model approximation (R4MA) [17, 18] (see the second row). The third and fourth rows of the table refer to the Monte Carlo simulation results [25] and experimental data [27], respectively

Research methods	Na			K		
	kT_c	$\bar{n}_c$	P_c	kT_c	$\bar{n}_c$	P_c
Theory (CFM, ZMA)	5.760	0.997		5.037	0.935	
Theory (CFM, R4MA)	4.028	0.997	0.474	3.304	0.935	0.408
Simulations	5.874	1.430	2.159	5.050	1.125	1.651
Experiment	3.713	1.215	0.415	3.690	0.772	0.498

The latter relation allows us to express the chemical potential in terms of the average number of particles $\bar{N}$ or in terms of the average density

$$\bar{n} = \frac{\bar{N}}{N_v} = \left(\frac{\bar{N}}{V}\right) v, \tag{14}$$

where v is the volume of a cubic cell. Combining Eqs. (12) and (13), we find the pressure P as a function of the temperature T and the average density $\bar{n}$, in other words, the equation of state of our model.

The equation of state of the cell fluid model at $T > T_c$ obtained using the simplest non-Gaussian quartic fluctuation distribution (the ρ^4 model), takes the form [17]

$$\frac{Pv}{kT} = P_a^{(+)}(T) + E_\mu + \left(\frac{\bar{n} - n_g}{\sigma_{00}^{(+)}}\right)^6 \times$$

$$\times \left[e_0^{(+)} \frac{\alpha}{(1+\alpha^2)^{1/2}} + \gamma_s^{(+)} - e_2^{(+)}\right]. \tag{15}$$

The quantity $P_a^{(+)}(T)$ appearing in Eq. (15) contains an analytic dependence on the temperature. The coefficient $\gamma_s^{(+)}$ characterizes the nonanalytic contribution to the thermodynamic potential. The quantities $e_0^{(+)}$, $e_2^{(+)}$, and $\sigma_{00}^{(+)}$ depend on the roots of a specific cubic equation. The expressions for all these quantities, as well as for E_μ, are given in [17]. Using Eq. (15), in Fig. 2, we demonstrate the pressure behavior as the density increases.

4. Critical Point Parameters of Fluids and Thermodynamic Coefficients

The proposed analytic approach, developed to describe the critical behavior of the cell fluid model by accounting for the non-Gaussian fluctuations of the order parameter (the ρ^4 model approximation), is applied to the Morse potential parameters characteristic of simple alkali metals (sodium and potassium). The critical point temperature kT_c can be calculated using the equation obtained in our paper [17]. Eqs. (10) and (15) give expressions for the critical fluid density $\bar{n}_c$ and pressure P_c, respectively. Table shows the numerical estimates of the critical point parameters, which we obtained for sodium and potassium. The results of the so-called zero mode approximation (the mean-field approximation) (see [26]) are in the first row, and those based on the proposed theory (see [17, 18] and this paper) are in the second row. For comparison, Table also contains the results of other authors.

The zero mode approximation does not account for the fluctuations of the order parameter. This approximation is inefficient near the critical point, where fluctuation effects play a significant role. The ρ^4 model approximation involves the non-Gaussian order parameter fluctuations that lead to the emergence of a RG symmetry. Table allows the evaluation of the discrepancies between theoretical, experimental, and Monte Carlo simulation results. As can be seen from Table, our estimates of the critical point parameters for Na and K in the ρ^4 model approximation agree better with the experimental data [27] than the numerical results [25] obtained by Monte Carlo simulations. The critical temperatures for Na and K are overestimated in Monte Carlo calculations. The

critical pressures for the alkali metals show significant deviations from theoretical and experimental values. For Na, the pressure is vastly overestimated, because the critical temperature is overvalued. It is observed that, at the experimental critical point of Na metal, 2485 K, the corresponding pressure predicted by simulation is a good approximation to the experimental critical pressure. In [25], the authors noted that the critical properties of Na and K are overestimated by their simulations, which means that the used parameters need to be refined to give a better agreement with experimental data. Scaling of the parameters to correctly predict the literature values, which are also observed to have a wide scatter, is reserved for a further study.

Using the equation of state (15), we can calculate and investigate thermodynamic coefficients (isothermal compressibility, density fluctuations, and thermal expansion) in the supercritical temperature region ($T > T_c$).

The subsequent figures illustrate the results of our numerical calculations obtained for sodium in a vicinity of the critical point. Figure 3 demonstrates the density dependence of the isothermal compressibility

$$K_T = \frac{1}{\eta}\left(\frac{\partial\eta}{\partial\tilde{p}}\right)_T = \frac{P_c}{\bar{n}}\left(\frac{\partial P}{\partial\bar{n}}\right)_T^{-1} \tag{16}$$

for fixed temperature values (we used the same values of τ to plot the isotherms in Fig. 2). Here, $\eta = \bar{n}/\bar{n}_c$, $\tilde{p} = P/P_c$. Proceeding from the extreme values of the isothermal compressibility K_T (the dashed line in Fig. 3), we can construct the Widom line of the supercritical cell fluid (see Fig. 4). The density fluctuations

$$\zeta_T = t\left(\frac{\partial\eta}{\partial\tilde{p}}\right)_T = \frac{P_c(1+\tau)}{\bar{n}_c}\left(\frac{\partial P}{\partial\bar{n}}\right)_T^{-1} \tag{17}$$

and the thermal expansion coefficient

$$\alpha_P = -\frac{1}{\eta}\left(\frac{\partial\eta}{\partial t}\right)_P = -\frac{1}{\bar{n}}\left(\frac{\partial\bar{n}}{\partial\tau}\right)_P, \tag{18}$$

calculated in addition to the isothermal compressibility, are shown in Figs. 5 and 6, respectively. Here, $t = T/T_c$.

The graphs in Figs. 3 and 5 are similar to each other, since the behavior of K_T and ζ_T is determined by the same derivative $(\partial P/\partial\bar{n})_T$ [see Eqs. (16) and (17)].

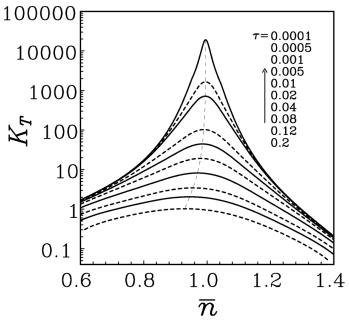

Fig. 3. Evolution of the isothermal compressibility with increasing density for various values of the relative temperature

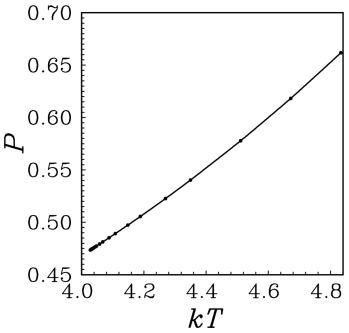

Fig. 4. Pressure at the extreme points of the compressibility as a function of the temperature

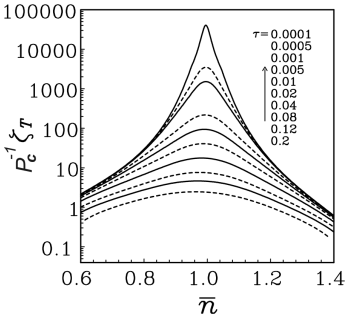

Fig. 5. Density fluctuations for temperatures close to the critical temperature

It should be noted that our calculations are valid in a small neighborhood of T_c, where theoretical and experimental researches are difficult to carry out. The solutions of recurrence relations (see [17]) allow us to calculate the size of the critical region. In these solutions, the terms proportional to E_3^n describe the entry to the critical regime, and the terms proportional to E_2^n describe the exit from the critical regime. Here, E_2 and E_3 are the eigenvalues of the RG linear transformation matrix, and n is the layer number in the

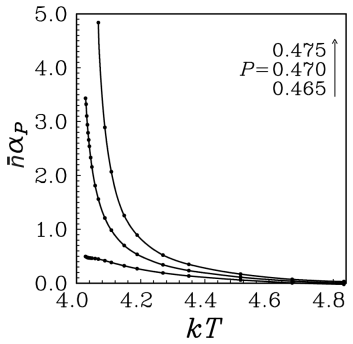

Fig. 6. Dependence of the thermal expansion α_P on the temperature for various fixed values of the pressure P

CV phase space. We can determine the temperature range $\tau < \tau^*$ in which the critical regime emerges using the solutions of recurrence relations and the condition for the critical regime existence (the exit from the critical regime for $n \to 1$ does not prevail over the entry to this regime). The temperature τ^* equals the magnitude of the smallest root of two equations obtained from solutions of the recurrence relations. The quantity τ^* determined in this way is of the order of a few hundredths ($\tau^* = 0.04$ in the case of liquid sodium, and $\tau^* = 0.02$ for potassium). The region of interest for most applications of supercritical fluids covers this temperature value (usually $1 < T/T_c < 1.1$ (or $0 < \tau < 0.1$) and $1 < P/P_c < 2$ [28]).

5. Conclusions

The behavior of the fluid system has been studied within the cell model in the immediate vicinity of the critical point. The region in a vicinity of the critical point is of interest (due to the fundamental and applied aspects) and difficult (due to the essential role of fluctuation effects) to analyze.

The method developed by us in [17] for Morse fluids has been applied to describe the phase transition in simple liquid alkali metals. The calculations have been performed for the parameters of the Morse interaction potential, which are related to alkali metals (sodium and potassium). We have calculated the critical point parameters for sodium and potassium, which are in agreement with the experimental data. The equation of state of the cell fluid model allowed us to obtain the pressure as a function of the temperature and density, as well as to study the behavior of thermodynamic coefficients (isothermal compressibility, density fluctuations, and thermal expansion) for sodium in the supercritical temperature region.

We see from Fig. 2 that the isotherms acquire a flat portion in the immediate vicinity of the critical point, i.e., the slope $(\partial P/\partial\bar{n})$ goes to zero at $T \longrightarrow T_c^+$. This corresponds to the fact that the isothermal compressibility (16) and the density fluctuations (17) become very large, when approaching the critical point (see Figs. 3 and 5). Very large values of the isothermal compressibility mean that the sensitivity of the density to very small pressure fluctuations is very large. The extreme values of the isothermal compressibility found in the case of sodium are used to construct the Widom line (see Fig. 4). The latter is the boundary between the gaseous and liquid structures of the supercritical fluid.

The behavior of the temperature-dependent thermal expansion at a fixed pressure is shown in Fig. 6. For various fixed pressures, we see a decrease in the thermal expansion coefficient (18) with increasing supercritical temperature, which is typical of gases. The thermal expansion coefficient of gases with increasing temperature approaches the value of the thermal expansion coefficient of an ideal gas, which is equal to the reciprocal absolute temperature.

We hope for that our approach to simple fluid systems may provide useful benchmarks in studying the critical behavior of multicomponent fluids. The conducted research also provides a certain methodological contribution to the theoretical description of critical phenomena.

1. C.-L. Lee, G. Stell, J.S. Høye. A simple SCOZA for simple fluids. *J. Mol. Liq.* **112**, 13 (2004).
2. C.E. Bertrand, J.F. Nicoll, M.A. Anisimov. Comparison of complete scaling and a field-theoretic treatment of asymmetric fluid criticality. *Phys. Rev. E* **85**, 031131 (2012).
3. A. Parola, L. Reatto. Recent developments of the hierarchical reference theory of fluids and its relation to the renormalization group. *Mol. Phys.* **110**, 2859 (2012).
4. A.V. Chalyi, L.A. Bulavin, V.F. Chekhun, K.A. Chalyy, L.M. Chernenko, A.M. Vasilev, E.V. Zaitseva, G.V. Khrapijchyk, A.V. Siverin, M.V. Kovalenko. Universality classes and critical phenomena in confined liquid systems. *Condens. Matter Phys.* **16**, 23008 (2013).
5. I.R. Yukhnovskii. The phase transition of the first order in the critical region of the gas-liquid system. *Condens. Matter Phys.* **17**, 43001 (2014).
6. T.J. Yoon, Y.-W. Lee. Current theoretical opinions and perspectives on the fundamental description of supercritical fluids. *J. Supercrit. Fluids* **134**, 21 (2018).

7. L.F. Vega. Perspectives on molecular modeling of supercritical fluids: From equations of state to molecular simulations. Recent advances, remaining challenges and opportunities. *J. Supercrit. Fluids* **134**, 41 (2018).
8. A. Oleinikova, L. Bulavin, V. Pipich. Critical anomaly of shear viscosity in a mixture with an ionic impurity. *Chem. Phys. Lett.* **278**, 121 (1997).
9. S. Pittois, B. Van Roie, C. Glorieux, J. Thoen. Thermal conductivity, thermal effusivity, and specific heat capacity near the lower critical point of the binary liquid mixture n-butoxyethanol–water. *J. Chem. Phys.* **121**, 1866 (2004).
10. R. Marr, T. Gamse. Use of supercritical fluids for different processes including new developments–a review. *Chem. Eng. Process.* **39**, 19 (2000).
11. S. Artemenko, P. Krijgsman, V. Mazur. The Widom line for supercritical fluids. *J. Mol. Liq.* **238**, 122 (2017).
12. Y.X. Pang, M. Yew, Y. Yan *et al.* Application of supercritical fluid in the synthesis of graphene materials: A review. *J. Nanopart. Res.* **23**, 204 (2021).
13. A.R.H. Goodwin, J.V. Sengers, C.J. Peters. *Applied Thermodynamics of Fluids* (Royal Society of Chemistry, 2010) [ISBN: 978-1-84755-806-0].
14. M.A. Anisimov. *Critical Phenomena in Liquids and Liquid Crystals* (Gordon and Breach, 1991) [ISBN: 9782881248061].
15. D.Yu. Zalepugin, N.A. Tilkunova, I.V. Chernyshova, V.S. Polyakov. Development of technologies based on supercritical fluids. *Supercritical Fluids: Theory and Practice* **1**, 27 (2006) [in Russian].
16. M. Kozlovskii, O. Dobush. Representation of the grand partition function of the cell model: The state equation in the mean-field approximation. *J. Mol. Liq.* **215**, 58 (2016).
17. M.P. Kozlovskii, I.V. Pylyuk, O.A. Dobush. The equation of state of a cell fluid model in the supercritical region. *Condens. Matter Phys.* **21**, 43502 (2018).
18. I.V. Pylyuk. Fluid critical behavior at liquid–gas phase transition: Analytic method for microscopic description. *J. Mol. Liq.* **310**, 112933 (2020).
19. A.L. Rebenko. Cell gas model of classical statistical systems. *Rev. Math. Phys.* **25**, 1330006 (2013).
20. V.A. Boluh, A.L. Rebenko. Cell gas free energy as an approximation of the continuous model. *J. Mod. Phys.* **6**, 168 (2015).
21. I.V. Pylyuk, O.A. Dobush. Equation of state of a cell fluid model with allowance for Gaussian fluctuations of the order parameter. *Ukr. J. Phys.* **65**, 1080 (2020).
22. I.V. Pylyuk, M.P. Kozlovskii. First-order phase transition in the framework of the cell fluid model: Regions of chemical potential variation and the corresponding densities. *Ukr. J. Phys.* **67**, 54 (2022).
23. I.R. Yukhnovskii. *Phase Transitions of the Second Order. Collective Variables Method* (World Scientific, 1987) [ISBN-10: 9971500876, ISBN-13: 9789971500870].
24. I.R. Yukhnovskii, M.P. Kozlovskii, I.V. Pylyuk. *Microscopic Theory of Phase Transitions in the Three-Dimensional Systems* (Eurosvit, 2001) [in Ukrainian] [ISBN: 966-7343-26-X].
25. J.K. Singh, J. Adhikari, S.K. Kwak. Vapor–liquid phase coexistence curves for Morse fluids. *Fluid Phase Equilib.* **248**, 1 (2006).
26. M.P. Kozlovskii, O.A. Dobush, I.V. Pylyuk. Using a cell fluid model for the description of a phase transition in simple liquid alkali metals. *Ukr. J. Phys.* **62**, 865 (2017).
27. F. Hensel. Critical behaviour of metallic liquids. *J. Phys.: Condens. Matter* **2**, SA33 (1990).
28. C.A. Eckert, B.L. Knutson, P.G. Debenedetti. Supercritical fluids as solvents for chemical and materials processing. *Nature* **383**, 313 (1996).

Received 07.07.23

І.В. Пилюк, М.П. Козловський, О.А. Добуш

ТЕРМОДИНАМІЧНІ ВЕЛИЧИНИ
ПЛИНІВ МОРЗЕ В НАДКРИТИЧНІЙ ОБЛАСТІ

Із врахуванням негаусових флуктуацій параметра порядку та потенціалу взаємодії Морзе розраховано параметри критичної точки для рідких лужних металів (натрію і калію). Досліджено поведінку ізотермічної стисливості, флуктуацій густини та теплового розширення для натрію в надкритичній температурній області. Суттєве зростання ізотермічної стисливості та флуктуацій густини біля критичної точки вказує на значну чутливість густини до незначних флуктуацій тиску. Коефіцієнт теплового розширення для різних фіксованих значень тиску проявляє типове для газів зменшення із зростанням надкритичної температури. Зображено лінію Відома, яка розділяє газоподібну та рідиноподібну структури плину при температурах вище критичної. Зазначимо, що наші розрахунки справедливі у вузькому околі критичної точки, який є проблематичним для теоретичних та експериментальних досліджень.

Ключові слова: потенціал взаємодії Морзе, критична точка, термодинамічний потенціал, ізотермічна стисливість, флуктуації густини, теплове розширення.